

# Radiometric Characteristics of KOMPSAT EOC Data Assessed by Simulating the Sensor Received Radiance

Jeong-Hyun Kim, Kyu-Sung Lee and Du-Ra Kim

Inha University, Department of Geoinformatic Engineering

**Abstract :** Although EOC data have been frequently used in several applications since the launch of the KOMPSAT-1 satellite in 1999, its radiometric characteristics are not clear due to the inherent limitations of the on-board calibration system. The radiometric characteristics of remotely sensed imagery can be measured by the sensitivity of radiant flux coming from various surface features on the earth. The objective of this study is to analyze the radiometric characteristics of EOC data by simulating the sensor-received radiance. Initially, spectral reflectance values of reference targets were measured on the ground by using a portable spectro-radiometer at the EOC spectrum. A radiative transfer model, LOWTRAN, then simulated the sensor-received radiance values of the same reference target. By correlating the digital number (DN) extracted from the EOC image to the corresponding radiance values simulated from LOWTRAN, we could find the radiometric calibration coefficients for EOC image. The radiometric gain coefficients of EOC are very similar to those of other panchromatic optical sensors.

**Key Words :** KOMPSAT, EOC, Radiometric Sensitivity, Gain, Radiometric Calibration, LOWTRAN, Spectroradiometer.

## 1. Introduction

The Korea multi-purpose satellite (KOMPSAT-1), the first earth observing satellite in Korea, has been successfully providing remotely sensed imagery since the launch in December 1999. Electro-optical camera (EOC) is one of two imaging sensors loaded on the KOMPSAT-1. EOC was initially designed to provide high spatial resolution stereo-images for topographic mapping. EOC is a push-broom type scanner operating in panchromatic mode of the spectrum range between 510 and 730 nm. At nadir looking, it has about 17km

swath width with spatial resolution of approximately 6.6m (Lee *et al.*, 1998).

After the initial testing period, the EOC sensor has functioned in stable condition. Even through the EOC sensor is providing relatively clear-looking image, the basic referential data necessary to characterize the radiometric quality of the EOC image are obviously insufficient. Unlike many other satellite data, such as SPOT and Landsat ETM+, pixel values of EOC data cannot be converted to the absolute values of radiant energy.

In the optical remote sensing data, the relationship between the digital number (DN) output of a sensor and

---

Received 10 July 2002; Accepted 28 August 2002.

the absolute value of radiance is defined as:

$$L = G \cdot DN + O \quad (1)$$

L = sensor-received radiance

DN = corresponding sensor output in digital number

G = calibration gain coefficient

O = offset coefficients

The radiometric calibration coefficient G can be estimated by the dynamic range ( $L_{\max} - L_{\min}$ ) of a sensor and the depth of digital number (DN) value. In EOC data with the 8-bits depth of DN value, the calibration coefficient can be obtained by dividing the dynamic range ( $L_{\max} - L_{\min}$ ) by 255. Therefore, the gain coefficient can represent the sensitivity of radiance value for a DN output in the image (Belward *et al.*, 1991). Of course, the maximum and minimum radiance that the sensor can respond to must be known. The radiometric calibration of a sensor can be performed by several methods of the preflight laboratory works, the post-launch on-board calibration techniques, and the post-launch ground reference calibration (Thome, *et al.*, 1997). Because EOC sensor does not have the internal calibration mechanism, it is difficult to determine the radiometric calibration coefficient by the in-flight on-board calibration technique. The objective of this study is to estimate the radiometric calibration gain coefficient of the EOC sensor by using the ground reference method.

## 2. Methods

Since EOC does not have the on-board calibrators, it can be calibrated only by the ground-reference approach. The post-flight calibration using ground reference targets, often called as 'vicarious calibration', can be carried out by obtaining both radiance and DN values in equation (1). If we had sets of L and DN values from the ground reference targets, we could

calculate the gain coefficient through the process suggested by Schroeder (2000).

Although we can obtain the DN value of a ground reference target directly from EOC image data, it is difficult to find its corresponding radiance value. The radiance entering the optics of EOC can be explained in a simple equation as follow:

$$L = \rho \frac{ET}{\pi} + L_p \quad (2)$$

L = sensor-received radiance,

$\rho$  = spectral reflectance of target,

E = irradiance on the target,

T = atmospheric transmittance

$L_p$  = path radiance

To obtain the radiance value L of a reference target, we used a radiative transfer code. The absolute radiance value of a reference target was estimated by applying the field-measured reflectance ( $\rho$ ), atmospheric parameters, and sensor parameters to LOWTRAN radiative transfer model. The radiative transfer code calculates such components of T and  $L_p$  in equation (2) and simulates the radiance value received from EOC. By correlating the DN and radiance value, we can determine the gain coefficient. The overall procedure to estimate the calibration coefficient using the ground reference targets is shown in Fig. 1.

### 1) Field Spectral Measurements

A portable field spectroradiometer (GER-2600) was used to measure the spectral reflectance of the ground reference targets at the time of EOC image capture. Although the device can measure spectral reflectance, radiance and irradiance at the wavelength range of 400nm to 2500nm, we used only the wavelength range of EOC spectrum (510 ~ 730nm). The spectroradiometer has 1.5nm bandwidth, measuring the reflectance for a reference target at 147 spectral channels of EOC spectrum. We used the average of 147 spectral reflectance values as a reflectance for the reference

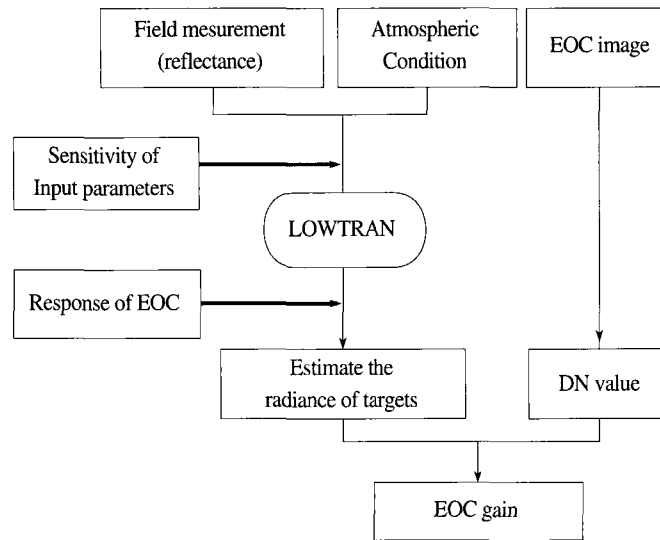


Fig. 1. Post-flight calibration approach to estimate the gain coefficient of EOC.

target.

The first field measurements were carried out at the Incheon International Airport on March 8, 2001 when the KOMPSAT-1 satellite actually passed over the study area. It was relatively clear sky with a few scattered clouds. Since it was the time when the airport was not yet opened, it provided several homogeneous fields (loading zone, runway, and other empty surfaces) for reference targets that were easily located on the EOC image. The second field measurements were conducted at the Munkyeong, Kyungsangbuk-do area on April 7, 2001. There was no EOC flight pass over the area at the time of field measurement. Because of the time gap between the field measurement and the EOC

image (obtained on June 5, 2000) at the Munkyeong site, the field measurements were primarily conducted on the invariant targets, such as quarry, concrete parking lot, and lake, in which the reflectance did not change over time. It was believed that reflectance of these targets was still useful for simulating radiance by LOWTRAN if we provided valid atmospheric parameters at the time of image acquisition. We measured four or five reference targets for each test site. To find the exact location of the field measurement, a global positioning system (GPS) was used. Table 1 shows the ground reference targets measured by the field spectrometer.

Table 1. Field Reflectance Measurements of Ground Reference Targets using Portable Spectroradiometer.

Test site	Incheon International Airport	Munkyeong, Kyungsanbuk-do
Measurement time	10:30 - 11:30 AM, March 8, 2001	10:00 - 12:00 AM, April 7, 2001
Corresponding EOC data acquisition	11:10 AM, March 8, 2001	10:43 AM, June 5, 2000
Reference targets	Loading zone Runway Grass Bare soil	Quarry Sand Lake Concrete parking lot

## 2) Simulation of Sensor-Received Radiance using LOWTRAN

The absolute value of radiance entering the optics of EOC was estimated by using a radiative transfer model. Radiative transfer models were frequently used to calibrate the radiometric performances of satellite sensors (Thome *et al.*, 1997; Castle *et al.*, 1984) and further to simulate the satellite signal in the solar spectrum (Vermote *et al.*, 1997). Radiative transfer models theoretically calculate the process of energy transfer and interaction between the earth surface and the satellite sensors. The model requires several input parameters related to the atmospheric condition, sun angles, earth-sun distance, and the sensor characteristics. With such input parameters, it calculates the amount of energy-matter interactions in atmosphere. Therefore, such models are often used for the atmospheric correction of remotely sensed images (Jang *et al.*, 1997).

LOWTRAN, developed by the United States Air Forces, was used in this study (Kneizys, *et al.*, 1988). The model calculates the major atmospheric interactions such as scattering, absorption, and refractions at various wavelengths. Among the input parameters to run LOWTRAN, the primary variables are related to the target reflectance, solar angles, atmospheric condition, and satellite and sensor specifications at the time of data acquisition. Before applying this model to EOC data, we

tested the performance of LOWTRAN by applying it to the SPOT data. Radiances of several reference targets on the SPOT image were obtained by applying the known calibration coefficients, and then compared with the radiance values estimated by LOWTRAN model. The results were very similar and it was believed that the LOWTRAN simulation of the sensor-received radiance was accurate enough for calculating the radiance for EOC sensor.

The model runs basically with six different types of atmospheric models such as tropical, mid-latitude summer, mid-latitude winter, sub-arctic summer, sub-arctic winter and 1976 US standard. Beside these basic atmospheric models, users can supply their own atmospheric model by incorporating the site-specific atmospheric data at the time of data acquisition. For this study, we used a separate atmospheric model that was constructed from the atmospheric data provided by a local meteorological station. To meet the input format of the LOWTRAN, atmospheric data of high altitude were interpolated from the existing data. Table 2 shows a few typical input parameters to run the LOWTRAN model. The sensitivity of each input parameter was also analyzed prior to the actual simulation of the EOC radiance. Among the several user-defined parameters such as atmospheric model, aerosol model, target altitude, and albedo, the aerosol model turned out to have greater influence than others.

Table 2. Example of LOWTRAN Input Parameters used for Incheon International Airport Site.

Atmospheric model	User specified model using atmospheric data collected at the time of data acquisition
Albedo	Field measured reflectance (%)
Aerosol model	Rural 5 Km
Season	Spring
Satellite altitude	685 km (KOMPSAT)
Target altitude	0 km
Azimuth angle	162.084 deg
Sensor angle from Sun	137.13 deg
Solar zenith angle	47.67 deg
Band width	510nm ~ 730nm

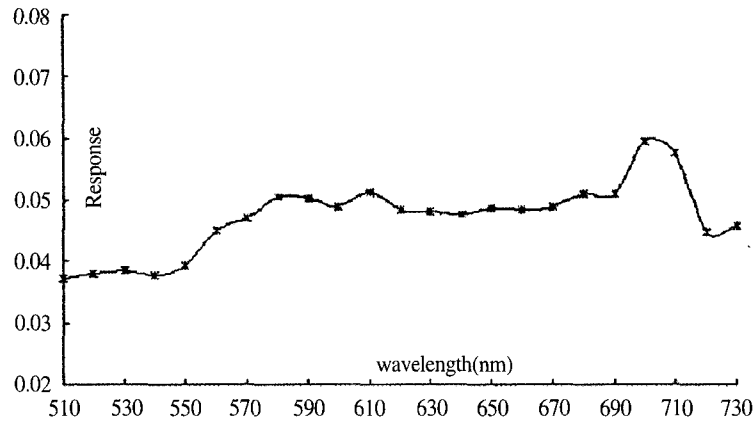


Figure 3. Spectral response of EOC spectrum at gain mode 4.

EOC is operated at the spectrum range between 510 nm to 730 nm. The spectral responsivity of the EOC detectors is not uniform throughout the EOC spectrum. Fig. 3 shows the responsivity of the EOC sensor at the gain mode 4, which is the currently operating mode (Lee *et al.*, 1998). It is clear that the incoming radiance at 700 nm has the highest sensitivity as compared with other wavelength. LOWTRAN simulates the EOC received radiance at about 1nm interval. Considering the differences in sensor responsivity, we integrated the LOWTRAN simulated radiance value by multiplying the spectral responsivity of the corresponding wavelength.

### 3) Extraction of Corresponding DN Values from EOC Images

Two EOC scenes were obtained for the test sites of the Incheon Airport and Munkyeong. The EOC images were geometrically registered to a plane rectangular coordinate system using a set of ground control points (GCP). After the registration of the EOC data, it was not difficult to find the exact location of the field measurement on the image. From the two EOC images

of Incheon and Munkyeong, digital number (DN) values of the ground measured targets were extracted. Each ground reference target was selected within a rather homogeneous field. We included several pixels surrounding the ground point and averaged them to obtain the DN value for the reference target to minimize the possible error in image registration. The DN value extracted from the EOC image was then compared with the corresponding radiance value that was simulated by LOWTRAN. The gain and offset coefficients were obtained from a simple regression model between DN and the simulated radiance.

## 3. Results and Discussions

Table 3 shows the field measured reflectance and the EOC received radiance values, simulated by LOWTRAN-7 model, of the ground reference targets at the Incheon International Airport and the Munkyeong. As defined by the equation (2), the relationship between the reflectance ( $\rho$ ) and the sensor-received radiance ( $L$ ) may or may not be linear. The difference between these two quantities depends on the atmospheric condition at the

Table 3. Field Measured Reflectance and LOWTRAN Estimated Radiance for Two Study Sites.

Test site		Field measured reflectance (%)	Simulated EOC radiance (watt/m <sup>2</sup> /μm/sr)
Incheon Airport	Loading zone	37.5	154
	Grass	13.5	97.1
	Runway	10.7	90.1
	Bare soil 1	22.5	116
	Bare soil 2	24.3	121
Munkyeong	Quarry	37.6	141
	Concrete pavement	36.2	136
	Lake	3.8	56.5
	Bare soil	32.3	126
	Sand	35.2	133

time of data acquisition.

Once we obtained the radiance values for all the ground reference targets and the corresponding DN values from the EOC image, we were able to estimate the gain coefficient. Gain and offset could be easily obtained from a simple regression function between the two variables. Gain, as a slope value in the graph, represents the equivalent radiance value corresponding to DN value 1. Fig. 3 shows the relationship between the DN value and radiance for the two study sites. On both sites, the relationship was very linear, even though the number of the reference targets was rather small.

The gain coefficients were 1.2253 at the Incheon Airport and 1.0532 at the Munkyeong. In both cases, the gain coefficients are not very different from each other when we considered the total amount of radiance that EOC could react to. The EOC image is recorded in 8-bit depth digital numbers. Therefore, the theoretical dynamic range of the EOC is from -17.3 w/m<sup>2</sup>/μm/sr to

295.2 w/m<sup>2</sup>/μm/sr for the Incheon site and is from -0.5 w/m<sup>2</sup>/μm/sr to 268.1 w/m<sup>2</sup>/μm/sr for the Munkyeong site. Although the EOC images can have DN values from 0 to 255, the actual range of DN values are rather narrow. Therefore, the differences in actual range of radiance received by EOC sensor might not be significant with such small difference in gain coefficients.

The estimated calibration coefficient of the EOC is very similar to those of other 8-bit depth satellite sensors. Table 4 compares the EOC gain coefficients with the Landsat ETM+ panchromatic channel (500~900nm) and the SPOT panchromatic channel (510~730nm). These sensors, as well as the EOC, are designed to operate at different gain modes in which the dynamic range of the sensor receiving radiance is altered. It seems that the current EOC gain coefficient (using the combined targets) mode is quite similar to the low gain mode of the ETM+ and SPOT sensors. In the

Table 4. Comparison of Gain Coefficients among Panchromatic Sensor.

Sensor	High gain mode		Low gain mode	
	Gain coefficient	Dynamic range (L <sub>min</sub> , L <sub>max</sub> )	Gain coefficient	Dynamic range (L <sub>min</sub> , L <sub>max</sub> )
EOC	-	-	1.0432	0.4, 266.5
ETM+ pan*	0.6392	-5, 158.4	0.9765	-5, 244.0
SPOT pan**	0.3497	0, 89.2	1.0	0, 255.0

\* <http://landsat7.usgs.gov/calibrations>

\*\* <http://www.spot.com/HOME/news/publi>

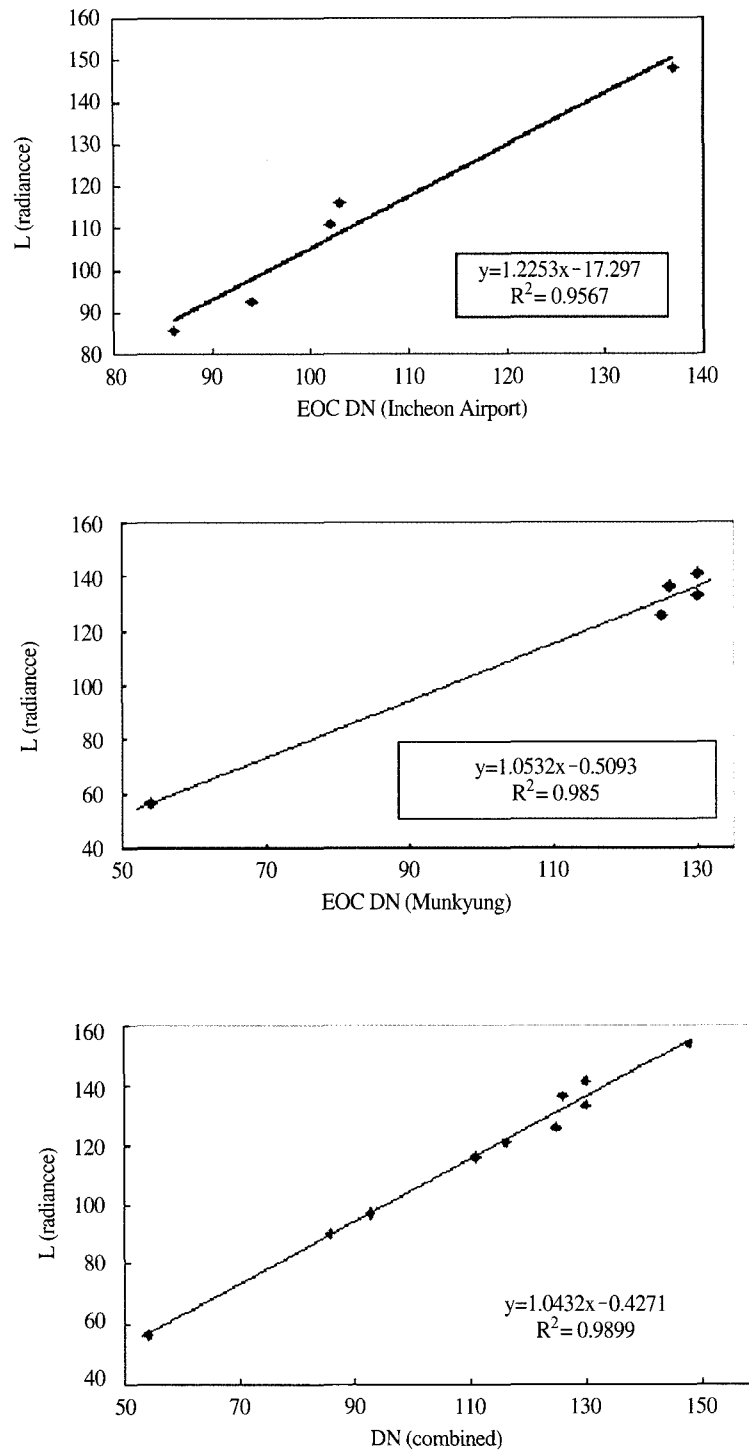


Figure 3. EOC gain coefficients estimated from the ground reference targets of each study site as well as from the combined targets of both sites.

low gain mode, DN value 1 is almost equivalent to  $1 \text{ W/m}^2/\mu\text{m/sr}$  of radiance. When the sensors are switched to the high gain mode, the sensor would have higher sensitivity with smaller gain coefficients. However, the sensor would have narrower dynamic range.

Although EOC does not have in-flight on-board calibration system to figure out the exact calibration coefficient to convert the DN value to the absolute radiance, it is considered to have a comparable radiometric performance. The estimated gain coefficients are close to 1.0, which means that the DN value in EOC images represents about the equal amount of incoming radiance of  $1 \text{ W/m}^2/\mu\text{m/sr}$ .

#### 4. Conclusions

In this study, we tried to assess the radiometric sensitivity of EOC by simulating the sensor-received radiance. Although the radiometric characteristic of EOC image could be analyzed in many different ways, the magnitude of the calibration coefficient can tell the dynamic range and the sensitivity of EOC sensor. We demonstrated a simple method to find the gain coefficient for EOC data by simulating the sensor-recorded radiance through the radiative transfer code, LOWTRAN. This approach is very similar to the post-launch vicarious calibration method in terms of using the ground reference targets. Spectral reflectance of the ground reference targets was measured at the time of image capture. By relating the DN value extracted from the EOC image to the radiance estimated by LOWTRAN, we could obtain the calibration coefficient for EOC.

The radiometric characteristics of EOC data have not been discussed very often because they are panchromatic images and are not designed to detect any surface features having subtle radiometric characteristics. Although EOC data would be primarily used for

topographic mapping, the radiometric quality of an image is still important in several aspects. For instance, EOC stereo images cannot be obtained simultaneously and their pixel values are very different from the radiometric behavior of the sensor system at the time of data acquisition.

This study showed a simple method to assess the radiometric performance of the EOC sensor. If we can estimate the actual radiance of diverse ground targets over various spatial and temporal scales, we can analyze the suitability of the gain mode setting and the dynamic range of EOC.

#### References

- Belward, A. S. and C. R. Valenzuela, 1991. *Remote Sensing and Geographical Information Systems for Resource Management in Developing Countries*, Boston, Kluwer Academic, pp. 97-110.
- Castle, K. R., R. G. Holm, C. J. Kastner, J. M. Palmer, P. N. Slater, Magdeleine Dinguirard, C. E. Ezra, R. D. Jackson and R. K. Savage, 1984. In-Flight Absolute Radiometric Calibration on the Thematic Mapper, *Proc. of 1984 IGARSS*, 2(3): 251-255.
- Jang, K.M., T.Y. Kwon and K.Y. Park, 1997. Study on the LOWTRAN-7 Simulation of the Atmospheric Radiative Transfer Using CAGEX data, *J. Korean Society of Remote Sensing*, 13(2): 99-120.
- Lee, S. H., H. S. Shim, and H.Y. Paik, 1998. Characteristics of the Electro-Optical Camera (EOC), *Proc. of 1998 Int. Symp. on Remote Sensing*.
- Kneizys, F. X., E. P. Shettle, L. W. Abreu, J. H. Chetwynd, G. P. Anderson, W. O. Anderson, J. E. A. Selby and S. A. Clough, 1988. *Users Guide to LOWTRAN 7*, AFGL-TR-0177, Air



- Force Geophysical Laboratory.
- Thome, K. J, B. L. Markham, J. L. Baker, P. N. Slater and S. F. Biggar, 1997. Radiometric Calibration of Landsat, *Photogrammetric Engineering and Remote Sensing*, 63(7): 853-858.
- Shroeder, M., R. Muller, P. Reinartz, M. Dingirard, L. Poutier and X. Briottet, 2000. Radiometric intercalibration of MOMS and SPOT by vicarious method, *International Archives of Photogrammetry and Remote Sensing*, 33(B1): 278-287.
- Vermote, E.F., D. Tanre, J.L. Deuze, M. Herman and J.-J. Morcrette, 1997. Second Simulation of the satellite signal in the solar spectrum, 6S: An Overview, *IEEE Transactions on Geoscience and Remote Sensing*, 35(3): 675-686.